Available online at www.sciencedirect.com
ScienceDirect
Journal of Magnetic Resonance 191 (2008) 120–127
JMR Journal of Magnetic Resonance
www.elsevier.com/locate/jmr

Exploiting the chemical shift displacement effect in the detection of glutamate and glutamine (Glx) with PRESS

Atiyah Yahya [a,b,*], Burkhard Mädler [c,d], B. Gino Fallone [a,b]

[a] Department of Medical Physics, Cross Cancer Institute, 11560 University Avenue, Edmonton, Alta., Canada T6G 1Z2
[b] Department of Oncology, University of Alberta, 11560 University Avenue, Edmonton, Alta., Canada T6G 1Z2
[c] Philips Medical Systems, University of British Columbia, 2221 Wesbrook Mall, Vancouver, BC, Canada, V6T 2B5
[d] Department of Physics and Astronomy, University of British Columbia, 2221 Wesbrook Mall, Vancouver, BC, Canada, V6T 2B5

Received 15 August 2007; revised 19 December 2007
Available online 25 December 2007

Abstract

A PRESS (Point RESolved Spectroscopy) sequence for the improved detection of the C_2 protons of Glx (glutamate and glutamine) at ≈3.75 ppm is presented in this work. It is shown that for spins like the C_2 protons of Glx which are involved solely in weak coupling interactions, the chemical shift displacement effect can be turned to advantage by exploiting PRESS refocusing pulses with bandwidths less than the chemical shift difference between the target spins and the spins to which they are weakly coupled. The narrow-bandwidth PRESS sequence allows refocusing of the *J*-coupling evolution of the target protons in the voxel of interest independently of echo time yielding signal equivalent to that which can be obtained with a one-pulse acquire sequence (assuming ideal pulses and ignoring T_2 relaxation). The total echo time of PRESS was set long enough for the decay of macromolecule signal and the two echo times were empirically optimized so that the Glx signal at 3.75 ppm suffered minimal contamination from myo-inositol. The efficacy of the method was verified on phantom solutions of Glx and on brain *in vivo*.

Keywords: PRESS; RF pulse bandwidth; Chemical shift displacement; Glutamate; Spectral editing

1. Introduction

Proton magnetic resonance spectroscopy (MRS) investigations have shown that changes in the collective levels of glutamate (Glu) and glutamine (Gln), often referred to as Glx, are relevant in the study of tumors as well as neurodegenerative and psychiatric diseases [1–6]. Commonly, a short echo time (TE) STimulated Echo Acquisition Mode [7], STEAM, or Point RESolved Spectroscopy [8], PRESS, sequence is employed for such MRS studies. While short-TE spectra yield more signal [9] because losses due to *J*-evolution are minimized, accurate Glx quantification from these spectra is challenging because all the Glx resonances suffer contamination from the macromolecule baseline signal [10] as well as from peaks of other metabolites. The signal from the C_4 Glx protons around 2.4 ppm is overlapped by signal from *N*-acetyl aspartate, NAA, and gamma-aminobutyric acid, GABA [11,12], and the C_2 Glx proton resonance around 3.75 ppm experiences some overlap with myo-inositol, mI [13]. A number of spectral editing techniques involving the PRESS sequence have been developed for Glx editing. Examples of these methodologies include TE-averaging [13], spectrally-selective refocusing [11], *J*-difference editing [14,15], optimized long-TE detection [16], and Carr–Purcell refocusing to minimize signal decay due to *J*-coupling evolution [17]. Most editing techniques resolve the peak of interest from undesired background at the expense of losing some signal from the target spins. The Carr–Purcell technique of Ref. [17], however, enabled the detection of coupled spins at long TEs, which is beneficial for eliminating the macromolecule

* Corresponding author. Address: Department of Medical Physics, Cross Cancer Institute, 11560 University Avenue, Edmonton, Alta., Canada T6G 1Z2.
E-mail address: ayahya@ualberta.ca (A. Yahya).

1090-7807/$ - see front matter © 2007 Elsevier Inc. All rights reserved.
doi:10.1016/j.jmr.2007.12.007

baseline, with almost no signal loss compared to a short-TE spectrum (apart from T_2 relaxation). However, the drawback of the sequence is that it requires a train of additional radiofrequency (RF) pulses and therefore care must be taken to be within SAR (specific absorption rate) guidelines, particularly at higher field strengths.

The objective of this work is to demonstrate an alternative method that can yield high Glx signal at long TEs without implementing any additional pulses to the basic PRESS sequence. The technique is applicable to spins that are involved solely in weak coupling; therefore, it is suitable for targeting the C_2 proton resonances of Glx. The idea is to employ a PRESS sequence with refocusing pulses that have bandwidths smaller than the chemical shift difference between the C_2 and C_3 protons of Glx. This ensures that the C_2 Glx protons are refocused in the voxel of interest while the C_3 protons to which they are weakly coupled are not, allowing the *J*-coupling evolution of the C_2 Glx protons to be "refocused" no matter what the PRESS echo time is. While the theory behind this is not new [18], the concept, to our knowledge, has not been previously exploited in the *in vivo* detection of Glx. We verified the efficacy of our method at 3 T on phantom solutions of Glu and Gln and *in vivo* on brain. In addition to employing a long TE to allow the decay of macromolecular signal contributions, the echo times of PRESS, namely, TE_1 and TE_2, were chosen such that contamination from mI was minimized. Although the method presented is limited in that it cannot resolve Glu from Gln, which would yield more biochemical information than measuring a collective Glx peak, it is a suitable alternative to short-TE PRESS and may potentially be applied in studies designed to determine whether or not Glx levels are of relevance in the diagnosis or treatment of an abnormality under investigation.

2. Theory

Glutamate and glutamine can each be represented as an *AMNPQ* spin system where the *A* spin (bonded to the C_2 carbon) is weakly coupled to the *M* and *N* protons (both bonded to the C_3 carbon). To gain an understanding of the evolution of the *A* proton during the PRESS sequence it is worthwhile to consider the response of a simpler weakly coupled AX_2 proton spin system, where the scalar coupling constant between the *A* and *X* spins is J_{AX}. Using product operator calculations, the evolution of spin *A* under the effect of the RF pulses (assumed to be ideal and non-slice-selective) and the scalar coupling interactions taking place during the time delays in the PRESS sequence can be calculated. To simplify calculations, the chemical shift evolution and its refocusing by the 180° pulses is ignored. The evolutionary terms are derived using standard transformations under RF pulse and scalar coupling Hamiltonians [19]. Considering only the response of the *A* spins, the sequence outcome can be derived to be $-A_Y\cos^2(\pi J_{AX}TE) + (2A_XX_{1Z} + 2A_XX_{2Z})\sin(\pi J_{AX}TE)\cos(\pi J_{AX}TE) + 4A_YX_{1Z}X_{2Z}\sin^2(\pi J_{AX}TE)$ describing how the signal is modulated as a function of TE under the influence of scalar coupling. If the bandwidth of the 180° refocusing pulses is reduced such that only the *A* spins are targeted by them then the outcome will be an optimum $-A_Y$. This situation can be achieved in a realistic PRESS sequence where the slice-selective pulses have a finite bandwidth by exploiting the chemical shift displacement effect. If the chemical shift difference between the *A* and *X* protons is δ_{AX} then the slice selected for spin *X* by a slice-selective pulse will be displaced by an amount $\frac{\delta_{AX}}{BW}\Delta x$ relative to the slice selected for spin *A*, where BW is the RF pulse bandwidth and Δx is the slice thickness. Employing refocusing pulses with bandwidths less than δ_{AX} will result in no overlap between the refocused *A* and *X* slices; therefore, only the *A* spins will experience the refocusing pulses in the voxel of interest and the result will be in-phase A_Y signal regardless of echo time.

3. Materials and methods

3.1. Numerical

To calculate the response of the C_2 protons of Glu and of Gln to a PRESS sequence at 3.0 T, a MATLAB program was implemented specifically to perform density matrix calculations for the *AMNPQ* proton spin systems of Glu and of Gln. Chemical shift, scalar coupling, and RF field interactions were taken into account. Ideal refocusing pulses were assumed and relaxation was not considered. The number of sampling points and spectral width used to simulate the acquisition period were the same as the experimental values. The five chemical shift (δ) and eight scalar coupling constants (*J*) were obtained from Ref. [20]. When simulating the application of the refocusing pulses exclusively to the *A* spins of Glu, the refocusing RF pulse Hamiltonian included only the *A* spin operators.

3.2. Experimental

Experiments were conducted with a 3 T Philips Intera scanner and a transmit/receive birdcage head coil. Water suppression was carried out by a CHESS module [21] composed of 110 Hz bandwidth pulses. It was experimentally verified that the CHESS pulses had negligible effect on spins resonating at frequencies that deviated by more than 95 Hz from the frequency at which the pulses were applied safely excluding the C_2 Glx protons and the creatine (Cr) peak at 3.9 ppm. For all experiments, a standard PRESS sequence, consisting of an excitation pulse and two refocusing pulses, was used. Two versions of the PRESS sequence were employed. In one version, the PRESS sinc refocusing pulses were of standard bandwidth (bandwidth ≈680 Hz, length ≈5.5 ms) and were designed to minimize the spatial extent of the tip-angle transition region. In the second version, the refocusing pulses were of the same shape but were 30.8 ms in length with a narrow-bandwidth of 121 Hz

which is much less than the chemical shift difference between the C_2 and the C_3 protons of Glu and Gln at 3 T (≈207 Hz). The minimum echo times achievable when using the pulses of small-bandwidth were $\{TE_1, TE_2\} = \{70\text{ ms}, 40\text{ ms}\}$. The offset frequency of the pulses was set to approximately 3.74 ppm. In all cases, the slice-selective PRESS pulses were applied in conjunction with gradients such that a $2 \times 2 \times 2\text{ cm}^3$ voxel was selected. Spoiler gradients of length 2.5 ms and strength 10 mT/m were applied prior to and after the refocusing pulses in three orthogonal directions. A four step phase cycling scheme was employed where the phase of the excitation pulse and that of the receiver were cycled through $\{x, y, -x, -y\}$. All spectra were acquired as 2048 complex data points sampled at a frequency of 2500 Hz. Phantom and *in vivo* spectra were acquired in 32 and 128 averages, respectively; and a repetition time of 3 s was used resulting in an acquisition time of about 6.8 min (including dummy scans) for one *in vivo* spectrum. Shimming was carried out by the built in Philips automatic iterative shimming procedure, and *in vivo* water peak linewidths were measured to be approximately 7–9 Hz. To minimize the amount of lipid signal appearing in the *in vivo* spectra as a result of the chemical shift displacement effect, the sequence was preceded by an outer volume suppression module which involved the excitation and dephasing of signal from four 30 mm slabs placed over the skull regions surrounding the targeted voxel.

The effects of the PRESS sequence with small-bandwidth refocusing pulses were examined with five different 6 cm diameter spherical phantom solutions of pH ≈ 7. All of the phantoms contained 10 mM Cr. Three of the phantoms contained only one other component, namely, 50 mM Glu, 50 mM Gln, and 50 mM mI. The other two phantoms were composed of mixtures based on physiological concentration ratios of gray matter of the human brain [22]; one contained 50 mM Glu and 23.9 mM Gln, and the other had the same constituents in addition to 31.1 mM mI. All chemicals were purchased from Sigma–Aldrich Canada. To find optimum timings for the small-bandwidth PRESS sequence that minimized Glx contamination from mI, thirty nine spectra were obtained from the 50 mM mI phantom with different $\{TE_1, TE_2\}$ echo time combinations, namely, $\{80\text{ ms}, 40\text{–}120\text{ ms}\}$, $\{90\text{ ms}, 40\text{–}110\text{ ms}\}$, $\{100\text{ ms}, 40\text{–}100\text{ ms}\}$, $\{110\text{ ms}, 40\text{–}90\text{ ms}\}$, $\{120\text{ ms}, 40\text{–}80\text{ ms}\}$, and $\{130\text{ ms}, 40\text{–}70\text{ ms}\}$, where TE_2 was incremented in steps of 10 ms.

3.3. Spectral quantification

The *in vivo* short-TE spectra were analyzed using LCModel (version 6.1) [23]. The basis set included spectra acquired from phantoms of aspartate (Asp), alanine (Ala), Cr, GABA, glucose (Glc), Glu, Gln, glycerophosphocholine (GPC), phosphocholine (PCh), lactate (Lac), mI, NAA, *N*-acetylaspartylglutamate (NAAG), scyllo-inositol (sIns), and taurine (Tau). Spectra for lipids and macromolecules were simulated using the default settings of LCModel. Spectra for lipids at 0.9 ppm (Lip09), 1.3 ppm (Lip13a–Lip13b), and 2 ppm (Lip20) were included in the basis set as well as spectra for macromolecules at 0.9 ppm (MM09), 1.2 ppm (MM12), 1.4 ppm (MM14), 1.7 ppm (MM17), and 2 ppm (MM20). The *in vivo* spectra were fitted in the range of 0.2 ppm and 4.2 ppm and the program reported metabolite concentrations relative to Cr. A sum for Glu + Gln (Glx) was also given. No corrections were made for relaxation.

For the spectra acquired by the method presented in this work the areas under the Glx peak (≈3.65 ppm to ≈3.85 ppm) and the Cr peak (≈3.85 ppm to ≈3.95 ppm) were calculated in MATLAB by summing the amplitudes of all points contributing to the peak of interest. The error in one amplitude measurement was assumed to be equal to half the peak-to-peak noise in the spectrum and this error was propagated through to calculate the errors in the peak areas and in their ratio. The areas were corrected for relaxation by dividing them by $e^{-TE/T_2}(1 - e^{-TR/T_1})$. The T_1 and T_2 values for the CH_2 protons of Cr at 3 T were taken to be 1020 ms and 128 ms, respectively [24]. For Glx, T_1 and T_2 values of 1230 ms (averaged over white and gray matter) and 200 ms, respectively, were assumed [25]. The area of Glx was also doubled to compensate for the difference in proton multiplicity of the molecular groups contributing to the Cr and Glx signal. In addition the Glx area was multiplied by a factor to correct for the small signal loss which results from the strong coupling interactions of the C_3 protons (see Section 4).

4. Results and discussion

The signal of the C_2 protons of Glu exhibits variation with changing echo time as a result of the weak scalar coupling interaction that exists between the C_2 and the C_3 protons. It was calculated (assuming ideal pulses) that the signal "refocuses" into an in-phase triplet when $TE_1 = TE_2 \approx 80$ ms, and this was experimentally verified by acquiring a spectrum from the entire 50 mM Glu phantom with a PRESS sequence ($TE_1 = TE_2 = 80$ ms) consisting of 750 μs rectangular pulses and no spatial localization gradients. The effect of a realistic PRESS sequence, where the excitation profiles of the refocusing pulses are imperfect and the chemical shift displacement effect comes into play, was demonstrated by acquiring a spectrum from an 8 cm^3 localized volume using the PRESS sequence described in Section 3.2 (refocusing pulse BW ≈ 680 Hz). The two spectra are displayed in Fig. 1(a) and were scaled such that the corresponding spectra (acquired with and without localization) obtained with TE = 30 ms had the same amplitude. It can be seen that the spectrum acquired with slice-selective pulses is ≈22% less in amplitude. Nevertheless, the contour plot in Fig. 5(b) of Ref. [26] calculated for the C_2 proton of Glu using the same 680 Hz bandwidth refocusing pulses employed in this work conveys that the resulting signal yield when $TE_1 = TE_2 = 80$ ms (≈70% of maximum ignoring relaxation) is the maximum achievable for echo times

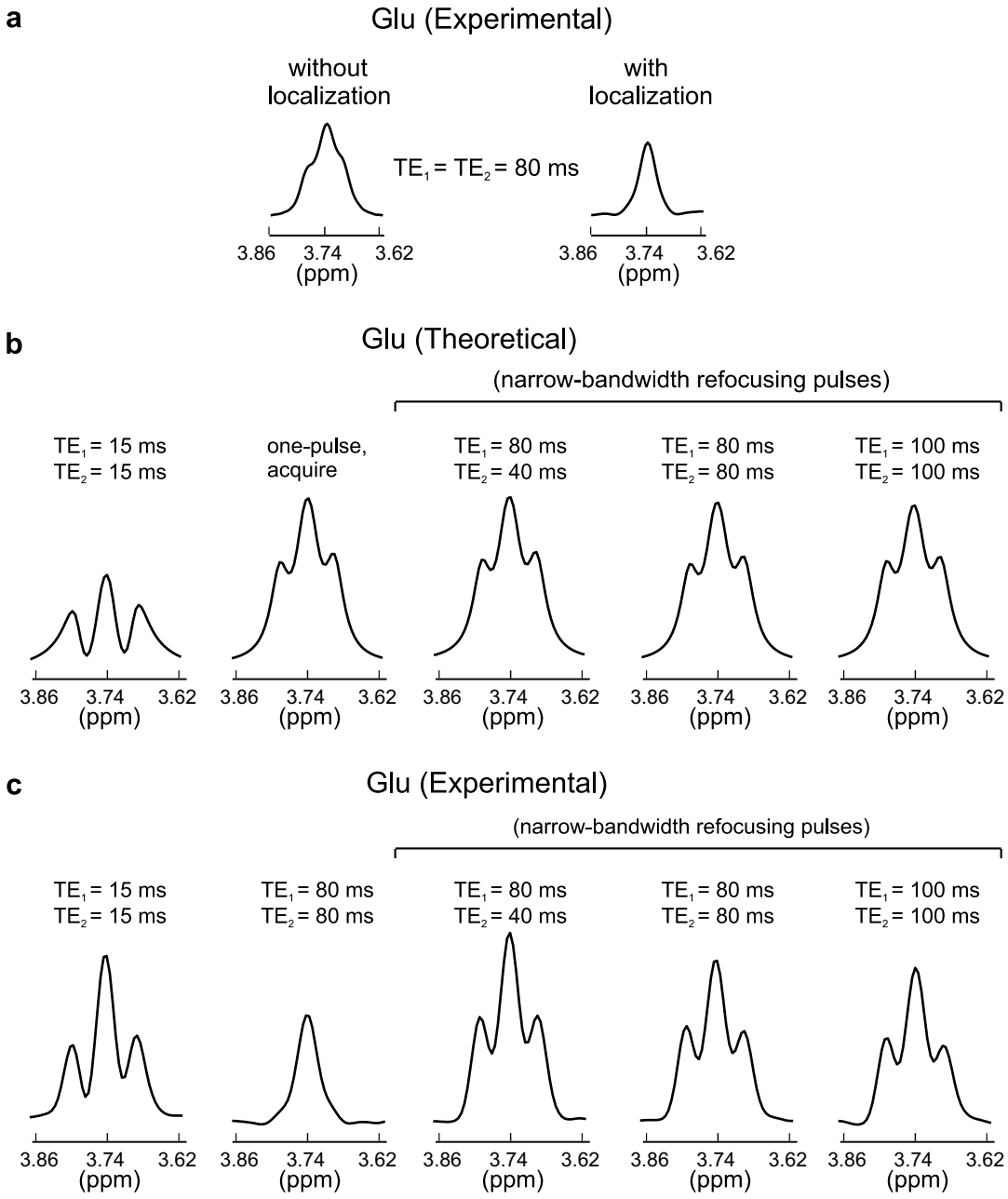

Fig. 1. The non-localized spectrum in (a) was acquired from the whole 50 mM Glu phantom with a PRESS sequence where the slice-selective pulses were replaced with 750 μs rectangular pulses and the spatial localization gradients were removed. The localized spectrum was obtained from a $2 \times 2 \times 2\ cm^3$ volume with a standard PRESS sequence (refocusing pulse BW ≈ 680 Hz). (b) The calculated response of the C_2 protons of Glu to a PRESS sequence with $TE_1 = TE_2 = 30$ ms, to a one-pulse acquire sequence, and to a PRESS sequence where the refocusing pulses target only the C_2 spins (labeled narrow-bandwidth refocusing pulses). Spectra obtained from a $2 \times 2 \times 2\ cm^3$ voxel from a 50 mM Glu phantom are displayed in (c). Employing the small-bandwidth refocusing pulses (121 Hz) results in an in-phase triplet for the C_2 protons of Glu as theoretically predicted. The effect of T_2 relaxation with increasing echo time is visible.

long enough for the decay of macromolecule signals (TE > 100 ms). The response of the C_2 proton of Gln is similar to that of Glu (see Fig. 5(c) of Ref. [26]). In this work, we demonstrate that the signal yield of the C_2 protons of Glx in response to a long-TE PRESS sequence can be significantly increased by exploiting refocusing pulses that have bandwidths less than the chemical shift difference between the C_2 and the C_3 protons as explained in Section 2. Fig. 1(b) shows the calculated response of the C_2 proton of Glu to a short-TE PRESS sequence (TE = 30 ms), to a one-pulse acquire sequence, and to PRESS sequences where the refocusing pulses exclusively target the C_2 proton. It is clear that the response to the latter situation yields as much signal as a one-pulse acquire experiment, namely, ≈65% and ≈75% more signal measured in terms of area and amplitude, respectively, relative to the short-TE PRESS sequence. The experimental outcome from experiments conducted on the 50 mM Glu

phantom is displayed in Fig. 1(c). A comparison between the two spectra obtained with $TE_1 = TE_2 = 80$ ms indicates that replacing the 680 Hz bandwidth refocusing pulses by the 121 Hz bandwidth pulses results in signal that is about 1.5 times larger in height and three fold greater in area. Calculations and experiments yielded similar results for Gln.

For minimal contamination of the Glx peaks from mI, it was found that $\{TE_1, TE_2\} = \{100\text{ ms}, 70\text{ ms}\}$ served as the most advantageous timings as demonstrated in Fig. 2(a). Fig. 2(b) displays a short-TE PRESS spectrum acquired from the 50 mM Glu/23.9 mM Gln/31.1 mM mI phantom where overlap of mI and Glx can be observed in the 3.7 ppm region. Applying the narrow-bandwidth PRESS sequence with optimized timings yields a triplet peak for Glx that does not suffer contamination from mI. This is verified by comparing the spectrum of Fig. 2(c) to one obtained from a phantom containing the same concentrations of Glu and Gln but no mI (Fig. 2(d)). To appreciate the signal gained by utilizing the refocusing pulses with small-bandwidth, a corresponding spectrum to the one shown in Fig. 2(d) was measured employing the regular refocusing pulses; see Fig. 2(e). The applicability of the sequence *in vivo* is demonstrated in Fig. 3. Spectra were acquired from the occipital lobes of three different normal volunteers. The voxels contained a mixture of gray and white matter. For each volunteer, a short-TE PRESS (TE = 30 ms) spectrum was measured in addition to a narrow-bandwidth PRESS spectrum (TE = 170 ms). Fig. 3(a) shows a short-TE PRESS spectrum acquired from one of

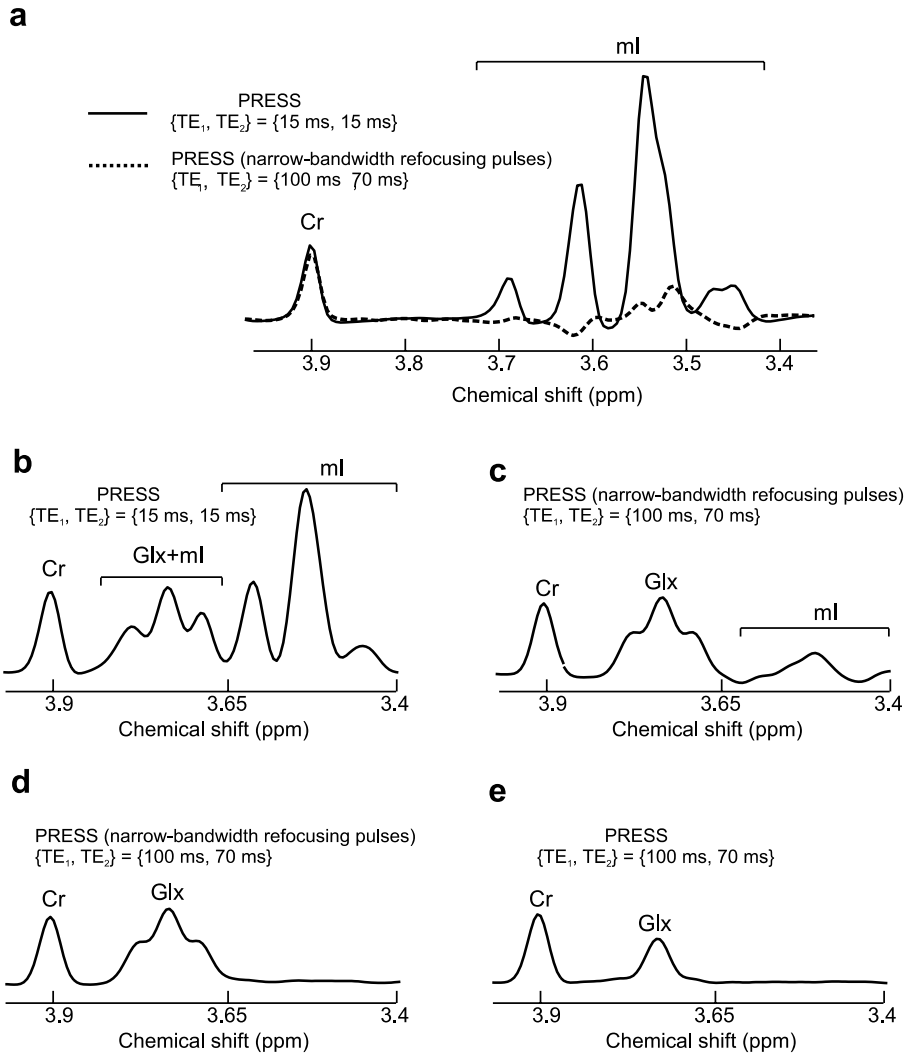

Fig. 2. The spectra in (a) were measured from a 10 mM Cr/ 50 mM mI phantom. The signal in the spectral region overlapping with Glx (3.65–3.7 ppm) is drastically reduced when using the small-bandwidth PRESS sequence with $\{TE_1, TE_2\} = \{100\text{ ms}, 70\text{ ms}\}$. Spectra (b) and (c) were obtained from a phantom composed of 10 mM Cr/50 mM Glu/ 23.9 mM Gln/31.1 mM mI. The overlap between Glx and mI observed in the short-TE PRESS spectrum in (b) is eliminated by the small-bandwidth PRESS sequence with optimized timings as can be seen by comparing the resulting Glx triplet in (c) with that acquired with the same sequence from a phantom containing the same amounts of Glu and Gln but no mI (d). The high Glx signal yield of the sequence is clearly visible when considering spectrum (d) versus spectrum (e) which was measured with the regular PRESS sequence with timings $\{TE_1, TE_2\} = \{100\text{ ms}, 70\text{ ms}\}$. The amplitude of the Glx peak in (d) is approximately 1.67 times larger than the one in (e). All voxel sizes were $2 \times 2 \times 2\text{ cm}^3$.

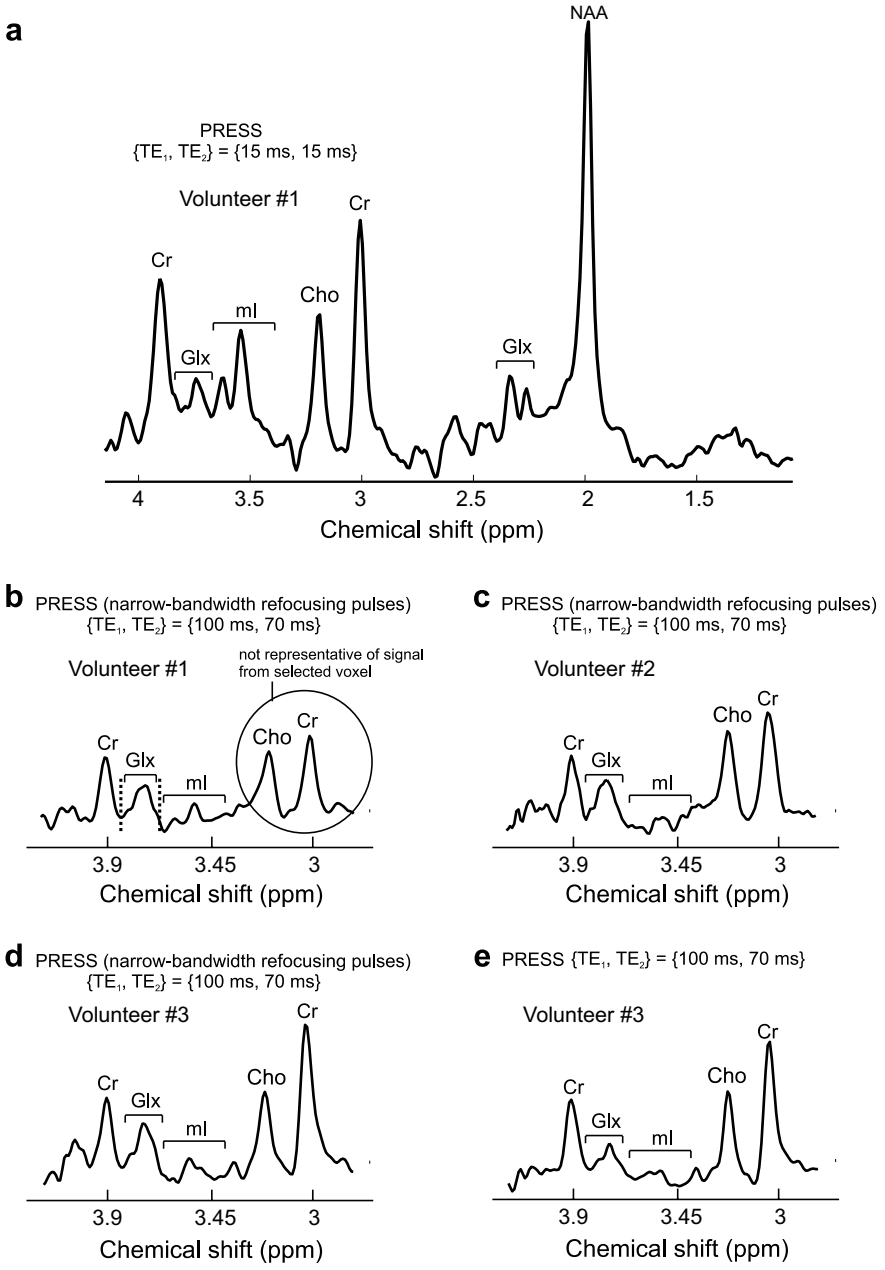

Fig. 3. Spectra were acquired from $2 \times 2 \times 2$ cm^3 volumes of the occipital lobes of three different volunteers. The overlap of macromolecule and mI signal with the C_2 proton peak of Glx can be observed in the short-TE PRESS spectrum of volunteer #1 shown in (a). The advantage of the narrow-bandwidth PRESS sequence is clear in (b) where a high Glx signal is yielded while the macromolecule baseline and mI signal have been suppressed. Narrow-bandwidth PRESS spectra obtained from the other two volunteers are displayed in (c) and (d). Spectrum (e) was acquired with the conventional PRESS sequence with $\{TE_1, TE_2\} = \{100\,\text{ms}, 70\,\text{ms}\}$ from the same voxel as in (d). Employing the low-bandwidth pulses increases the amplitude of the C_2 proton Glx peak by approximately a factor of 1.7.

the volunteers. The Glx peak in the 3.75 ppm region is clearly contaminated by mI and the macromolecule baseline. The benefit of employing the small-bandwidth PRESS sequence with optimized timings is exhibited in Fig. 3(b); high Glx signal is maintained, signal from mI is minimized, and the relatively long TE ensures the decay of the macromolecule baseline. The small-bandwidth PRESS spectra of the other two volunteers are displayed in Fig. 3(c) and (d). The spectrum in 3(e) was acquired with the conventional PRESS sequence with $\{TE_1, TE_2\} = \{100\,\text{ms}, 70\,\text{ms}\}$ from the same voxel as in (d). Comparing spectra (d) and (e) demonstrate that employing the low-bandwidth pulses increases the amplitude of the C_2 proton Glx peak by approximately a factor of 1.7. Admittedly, the Glx peak will suffer some contribution from the glutamate moiety of glutathione (GSH). Based on the chemical shift and scalar coupling constants given for GSH in Ref. [20] and on the Glu, Gln, and GSH gray matter concentrations listed in Ref. [22], it was calculated that $\approx$17.6% of the Glx peak could be attributed to GSH. Another drawback is that

because of the narrow bandwidths of the refocusing pulses (121 Hz in this case), information about most other metabolites from the targeted volume is lost. For example, the majority of the signal contributing to the choline (Cho) peak in Fig. 3(b)–(d) is not from the desired voxel but from a volume displaced by approximately 1.16 cm (see Eq. in Section 2) along both the x and y directions (directions of the refocusing pulse slice-selective gradients). By the same reasoning, the Cr peak at 3 ppm cannot play the role of an internal reference as it often does. However, the Cr peak at 3.9 ppm can serve this purpose since it is shifted by no more than $\approx$0.31 mm in the x and y directions relative to the selected voxel. While utilizing the 3.9 ppm Cr peak as a frequency and phase reference is straightforward, absolute quantification based on it requires taking into account its relaxation properties. As seen in Fig. 3(b), the Cr resonance at 3.9 ppm is significantly reduced as a result of T_2 relaxation. In fact, it has been determined that the Cr protons that resonate at 3.9 ppm have a T_2 that is shorter than that of the 3.0 ppm Cr protons by about 28% at 3 T [24]. Creatine is often used as a standard when estimating absolute metabolite concentrations [11,27]; however, in the presence of pathophysiology it cannot be assumed that the Cr concentration will remain unaltered. For example, it has been reported that Cr levels are elevated in patients with frontal lobe epilepsy [28]. In such cases, the ratio of Glx to Cr (relative quantification) may prove to be of more value than absolute quantification [29].

Although it is expected that the amplitude of the C_2 Glx signal in response to the narrow-bandwidth PRESS sequence will be independent of TE (apart from T_2 decay), it should be noted that small modulations in the signal intensity are present as a result of the C_3 protons being involved in strong scalar coupling interactions. We calculated the amplitude of the C_2 triplet of Glu at 14 different total echo times ranging between 120 ms and 1000 ms. The amplitudes were normalized to the maximum (set to 100%) and the mean and the standard deviation of the results were found to be 91.4% and 5.2%, respectively. For accurate quantification of the Glx signal the loss due to the strong coupling interactions of the C_3 protons need to be taken into account along with the losses due to relaxation. The correction factor for this loss was calculated to be 3.7% for the timings $\{TE_1, TE_2\} = \{100\text{ ms}, 70\text{ ms}\}$.

The ratio of the concentration of Glx to that of Cr is commonly determined by spectral fitting (for example by LCModel) of short-TE spectra that contain signal from the C_2, C_3, and C_4 protons of Glx. We employed LCModel to analyze the short-TE spectra acquired *in vivo* and we compared the output to the concentration ratios that we deduced from the corresponding spectra obtained by our presented technique (see Section 3.3 for analysis details). The results are summarized in Table 1 and the volunteer numbering is consistent with that of Fig. 3. It is clear that the ratios calculated from the long-TE spectra agree within error to the ratios provided by LCModel analysis of the short-TE spectra, justifying the reliability of Glx measurement from the C_2 peaks alone. The ratios also agree within error to values found in the literature [30]. The long-TE spectra could have also been evaluated by spectral fitting by creating a basis set consisting of line broadened spectra (to match *in vivo* linewidths) acquired from phantom solutions of Glu, Gln, mI, and Cr under the same sequence conditions and using a least squares algorithm as was done by Ref. [11].

Table 1
Summary of concentration ratios obtained from the short-TE PRESS spectra (LCModel fitting) and from the corresponding long TE, small-bandwidth PRESS spectra (direct integration of peaks)

Volunteer	[Glx]/[Cr] by LCModel analysis of short-TE spectrum	[Glx]/[Cr] by integration of peaks displayed in Fig. 3(b)–(d)
1	0.95 ± 0.12	0.96 ± 0.15
2	1.29 ± 0.15	1.25 ± 0.18
3	1.20 ± 0.14	1.16 ± 0.16

5. Conclusion

We demonstrate in this study a PRESS sequence that can yield high signal, comparable to that which can be achieved by a one-pulse acquire sequence, from the C_2 protons of Glx at long echo times which is favorable for the decay of macromolecule signal. The technique is applicable to spins whose scalar coupling interactions are limited to the weak coupling regime and it involves employing PRESS refocusing pulses that have bandwidths less than the chemical shift difference between the target spins and the spins to which they are weakly coupled. This renders the chemical shift displacement effect advantageous and allows refocusing of the J-evolution of the target signal in the voxel of interest regardless of the selected echo time. The technique also lends itself as a method for determining the T_2 relaxation constants of spins involved solely in weak coupling interactions.

Acknowledgments

We appreciate the financial support of the Canadian Foundation for Innovation (CFI) and the Alberta Science and Research Investment Program (ASRIP). We acknowledge Philips Medical Systems for research support and we also wish to thank the reviewers whose comments helped improve the quality of the manuscript.

References

[1] Y.D. Cho, G.H. Choi, S.P. Lee, J.K. Kim, 1H-MRS metabolic patterns for distinguishing between meningiomas and other brain tumors, Magn. Reson. Imaging 21 (2003) 663–672.
[2] G. Hasler, J.W. van der Veen, T. Tumonis, Reduced prefrontal glutamate/glutamine and gamma-aminobutyric acid levels in major depression determined using proton magnetic resonance spectroscopy, Arch. Gen. Psychiatry 64 (2007) 193–200.
[3] N. Hattori, K. Abe, S. Sakoda, T. Sawada, Proton MR spectroscopic study at 3 Tesla on glutamate/glutamine in Alzheimer's disease, Neurochemistry 13 (2002) 183–186.

[4] G. Helms, Volume correction for Edema in single-volume proton MR spectroscopy of contrast-enhancing multiple sclerosis lesions, Magn. Reson. Med. 46 (2001) 256–263.
[5] M. Rijpkema, J. Schuuring, Y. van der Meulen, M. van der Graaf, H. Bernsen, R. Boerman, A. van der Kogel, A. Heerschap, Characterization of oligodendrogliomas using short echo time 1H MR spectroscopic imaging, NMR Biomed. 16 (2003) 12–18.
[6] I. Savic, A.M. Thomas, Y. Ke, J. Curran, I. Fried, J. Engel, In vivo measurements of glutamine + glutamate (Glx) and *N*-acetyl aspartate (NAA) levels in human partial epilepsy, Acta Neurol. Scand. 102 (2000) 179–188.
[7] J. Frahm, K.-D. Merboldt, W. Hanicke, J. Magn. Reson. 72 (1987) 502–508.
[8] P.A. Bottomley, Selective volume method for performing localized NMR spectroscopy, US Patent 4,480,228, 1984.
[9] K. Zhong, T. Ernst, Localized in vivo human 1H MRS at very short echo times, Magn. Reson. Med. 52 (2004) 898–901.
[10] L. Hofmann, J. Slotboom, C. Boesch, R. Kreis, Characterization of the macromolecule baseline in localized 1H-MR spectra of human brain, Magn. Reson. Med. 46 (2001) 855–863.
[11] C. Choi, N.J. Coupland, P.P. Bhardwaj, N. Malykhin, D. Gheorghiu, P.S. Allen, Measurement of brain glutamate and glutamine by spectrally-selective refocusing at 3 Tesla, Magn. Reson. Med. 55 (2006) 997–1005.
[12] R.A. de Graaf, D.L. Rothman, Detection of gamma-aminobutyric acid (GABA) by longitudinal scalar order difference editing, J. Magn. Reson. 152 (2001) 124–131.
[13] R. Hurd, N. Sailasuta, R. Srinivasan, D.B. Vigneron, D. Pelletier, S.J. Nelson, Measurement of brain glutamate using TE-averaged PRESS at 3 T, Magn. Reson. Med. 51 (2004) 435–440.
[14] S.J. Mathew, P. Nestadt, X. Mao, C. Kelly, S. Levine, D.C. Shungu, Assessment of GABA and glutamate/glutamine using the *J*-edited spin echo difference method at 3 Tesla in patients with major depressive disorder, in: Proceedings of the 15th Annual Meeting of ISMRM, Berlin, 2007, p. 915.
[15] D.C. Shungu, X. Mao, L.S. Kegeles, Evaluation of GABA detection sensitivity gains achieved with an 8 channel phased-array head coil at 3.0 T in the human dorsolateral prefrontal cortex using the *J*-editing technique, in: Proceedings of the 14th Annual Meeting of ISMRM, Seattle, 2006, p. 488.
[16] F. Schubert, J. Gallinat, F. Seifert, H. Rinneberg, Glutamate concentrations in human brain using single voxel proton magnetic resonance spectroscopy at 3 Tesla, NeuroImage 21 (2004) 1762–1771.
[17] B.J. Soher, P.M. Pattany, G.B. Matson, A.A. Maudsley, Observation of coupled 1H metabolite resonances at long TE, Magn. Reson. Med. 53 (2005) 1283–1287.
[18] D.A. Yablonskiy, J.J. Neil, M.E. Raichle, J.J.H. Ackerman, Homonuclear *J* coupling effects in volume localized NMR spectroscopy: pitfalls and solutions, Magn. Reson. Med. 39 (1998) 169–178.
[19] R.R. Ernst, G. Bodenhausen, A. Wokaun, Principles of Nuclear Magnetic Resonance in One and Two Dimensions, Clarendon Press, Oxford, 1987.
[20] V. Govindaraju, K. Young, A.A. Maudsley, Proton NMR chemical shifts and coupling constants for brain metabolites, NMR Biomed. 13 (2000) 129–153.
[21] A. Haase, J. Frahm, W. Hanicke, D. Matthaei, 1H NMR chemical shift selective (CHESS) imaging, Phys. Med. Biol. 30 (1985) 341–344.
[22] R.A. De Graaf, D.L. Rothman, In vivo detection and quantification of scalar coupled 1H NMR resonances, Concepts Magn. Reson. 13 (2001) 32–76.
[23] S.W. Provencher, Estimation of metabolite concentrations from localized in vivo proton NMR spectra, Magn. Reson. Med. 30 (1993) 672–679.
[24] F. Traber, W. Block, R. Lamerichs, J. Gieseke, H.H. Schild, 1H metabolite relaxation times at 3.0 Tesla: measurements of T1 and T2 values in normal brain and determination of regional differences in transverse relaxation, J. Magn. Reson. Imaging 19 (2004) 537–545.
[25] S. Posse, R. Otazo, A. Caprihan, J. Bustillo, H. Chen, P.-G. Henry, M. Marjanska, C. Gasparovic, C. Zuo, V. Magnotta, B. Mueller, P. Mullins, P. Renshaw, K. Ugurbil, K.O. Lim, J.R. Alger, Proton echo-planar spectroscopic imaging of *J*-coupled resonances in human brain at 3 and 4 Tesla, Magn. Reson. Med. 58 (2007) 236–244.
[26] H. Kim, R.B. Thompson, C.C. Hanstock, P.S. Allen, Variability of metabolite yield using STEAM or PRESS sequences in vivo at 3.0 T, illustrated with myo-inositol, Magn. Reson. Med. 53 (2005) 760–769.
[27] I.-Y. Choi, S.-P. Lee, H. Merkle, J. Shen, Single-shot two-echo technique for simultaneous measurement of GABA and creatine in the human brain in vivo, Magn. Reson. Med. 51 (2004) 1115–1121.
[28] N. Lundbom, E. Gaily, K. Vuori, R. Paetau, E. Liukkonen, J.C. Rajapakse, L. Valanne, A.-M. Hakkinen, M.-L. Granstrom, Proton spectroscopic imaging shows abnormalities in glial and neuronal pools in frontal lobe epilepsy, Epilepsia 42 (2001) 1507–1514.
[29] J.F.A. Jansen, W.H. Backes, K. Nicolay, M.E. Kooi, 1H MR spectroscopy of the brain: absolute quantification of metabolites, Radiology 240 (2006) 318–332.
[30] R.A. de Graaf, In Vivo NMR Spectroscopy: Principles and Techniques, John Wiley & Sons, Toronto, 2002, p. 400.